J. Fluid Mech. (1978), *vol.* 85, *part* 3, *pp.* 459–477
Printed in Great Britain

Towards an optimum yacht sail

By C. J. WOOD AND S. H. TAN
Department of Engineering Science, University of Oxford

(Received 17 November 1976 and in revised form 22 June 1977)

This paper contains a simple and entirely conventional application of lifting-line theory to a close-hauled, high aspect ratio sail, set upright on a flat water surface. In seeking an optimum spanwise loading distribution however, an unconventional criterion is used, which leads to an unexpected result.

By seeking to maximize the forward thrust for a given rolling moment, rather than maximizing the lift–drag ratio, an optimum loading distribution is obtained which departs dramatically from elliptic loading. It offers the prospect of a significant improvement in extreme yacht performance if the associated mechanical and control problems can ever be solved.

1. Introduction

As the designers of sailing craft have sought to improve performance, particularly in sailing to windward, empirical experience has been complemented by the increasing application of modern aerodynamic knowledge. Much of this knowledge is the direct result of early research into the design of aeroplane wings. In some cases the similarities are sufficient to justify the direct application of the results and conclusions without the need for a fresh and fundamental theoretical analysis. Thus, for example, the attempt to produce sails of increasingly high aspect ratio with elliptical planform and reduced twist is a direct imitation of these features of aeroplane wing design which are known to produce optimum performance.

Sometimes this approach has yielded beneficial results. It is usually true, for example, that an improved lift–drag ratio leads to better windward performance. However, it is surely legitimate to question whether it is invariably true that what is beneficial for aeroplanes is also necessarily good for sailing yachts.

An aeroplane designer and operator wish to maximize the lift–drag ratio because in this way the cost of a given journey is minimized. If the aim of the yachtsman or yacht designer is questioned at the same basic level, one logical answer is that he wishes to travel as fast as possible without capsizing. When the wind is light and the risk of capsizing or excessive heeling is absent, then the vector diagrams of the force acting on a sail show without doubt that the highest lift–drag ratio gives the best performance *for a given sail area*. However, if the yacht is not about to capsize then it must be capable of carrying a larger sail with a consequent increase in forward thrust. The simple optimization of the lift–drag ratio has therefore not yielded maximum performance. Such a simple optimization is appropriate only when externally applied constraints, such as class rules, or the practical requirements of a safe and seaworthy craft, inhibit the search for a truly optimum design.

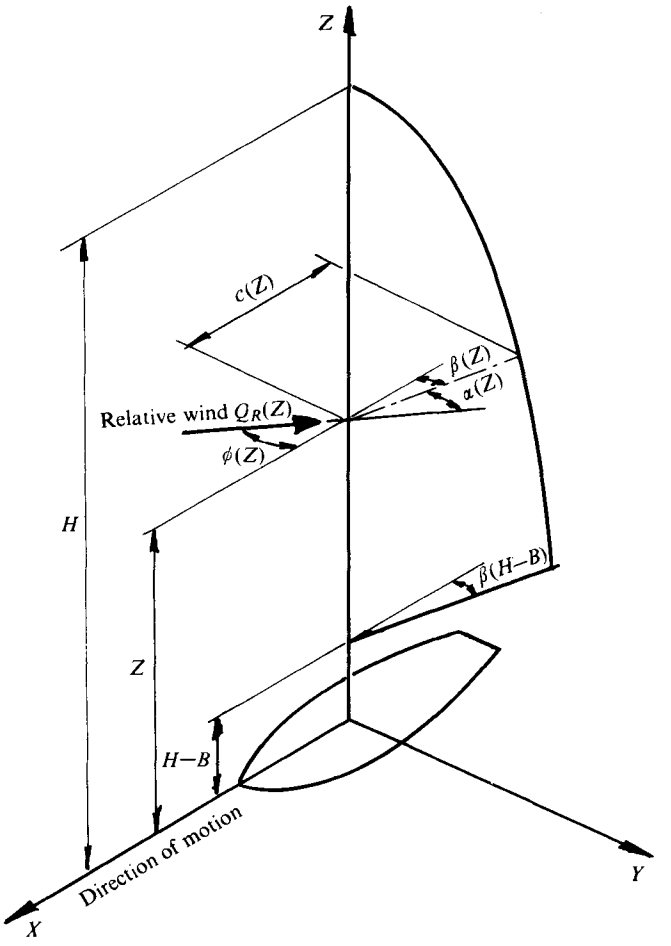

FIGURE 1. Definition of axes and principal dimensions.

This paper puts forward the proposal that the criterion for true optimization of windward performance of a sailing craft is not the maximization of the lift–drag ratio but is simply *the achievement of the greatest possible forward thrust without exceeding a given rolling moment.*

If this proposal is accepted, then the conventional results of aeroplane wing theory must be rejected and a new application of the theory must be made in order to seek for a design which satisfies the revised optimization condition.

The method of analysis employed is classical lifting-line theory. One reason for this unrealistic choice is historical. Inasmuch as it was lifting-line theory which led to the wide acceptance of a particular spanwise loading distribution (elliptic loading), so it is fitting to use the same theory in order to show by comparison, directly and in the same terms, the benefits in performance which may result from the adoption of the more basic optimization criterion proposed here.

The particular areas where the analysis is inadequate will be pointed out formally as they arise in the following paragraphs. It must be acknowledged that, because of these inadequacies, neither the time-honoured result nor the new optimum loading is

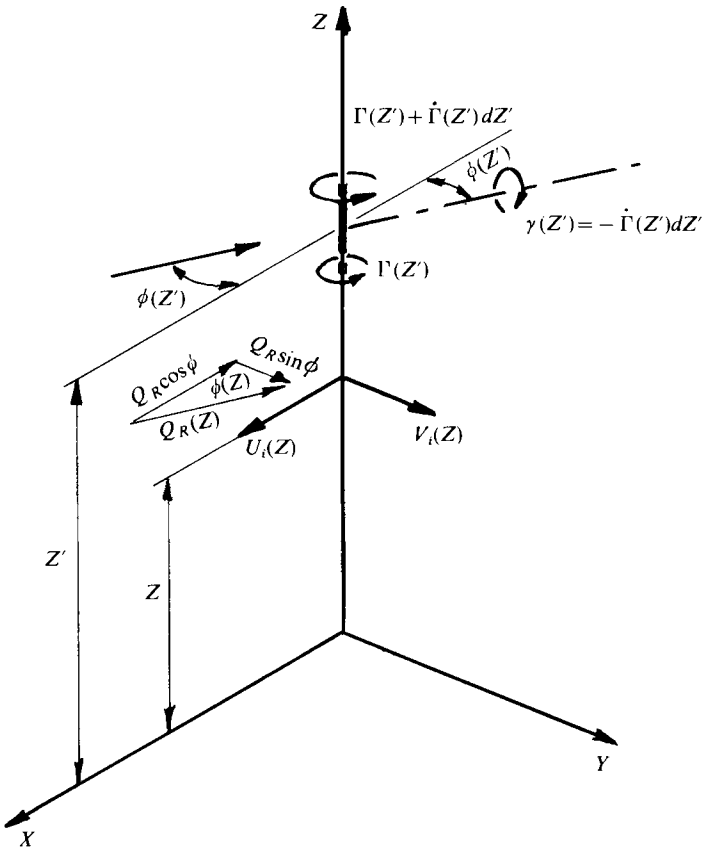

FIGURE 2. Notation and sign conventions for the application of lifting-line theory to a vertical sail.

realistic. Nevertheless, just as the old result provided an incentive to designers who were able to achieve a practical benefit under the influence of a simple theoretical idea, so it is hoped that the present paper may provide the initial motivation for those who may find themselves able to pursue the inquiry either by a more sophisticated theory, by experiment or by a study of the practical design problems.

2. The lifting-line model applied to a vertical sail

The application of lifting-line theory to a sail is of course not original. Both Tanner (1965) and Milgram (1968) have made use of this model with rather different objectives. The following analysis is also set out in detail by Wood & Tan (1976).

2.1. *General description*

In figure 1 a right-handed co-ordinate system is defined in which the X, Y plane coincides with the water surface with the X axis aligned parallel to the centre-line of the yacht hull and facing forwards. The Z axis is vertically upwards at the position of the sail. This is considered to be of high aspect ratio and is represented in figure 2 by a vortex line of variable strength $\Gamma(Z)$ on the Z axis.

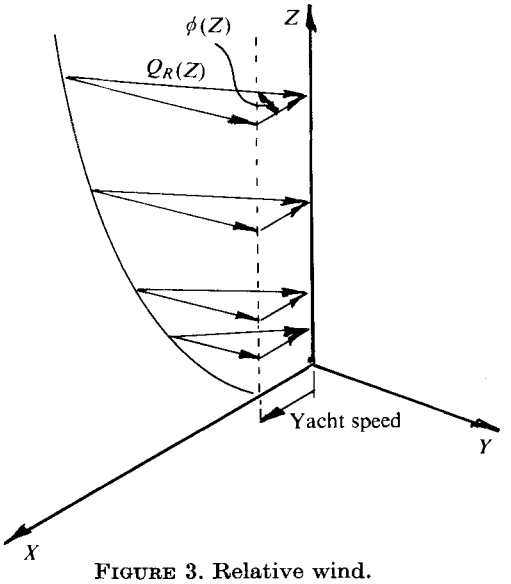

FIGURE 3. Relative wind.

The variation in $\Gamma(Z)$ gives rise to a trailing vortex sheet of strength $\gamma_T(Z)$. The sign convention chosen for $\Gamma(Z)$ and $\gamma_T(Z)$ is the right-hand screw convention, so that $\gamma_T(Z)$ is given by

$$\gamma(Z) = -d\Gamma(Z)/dZ = -\dot{\Gamma}(Z). \tag{1}$$

It is assumed that the trailing vortex sheet will be aligned at every height Z with the local relative wind vector $\{Q_R(Z), \phi(Z)\}$, which is the resultant of the undisturbed wind vector and the motion of the yacht through the water (figure 3). If the wind were uniform, then $\phi(Z)$ would not vary with height. In general, however, if the absolute wind speed near the water surface is reduced by friction, and even if the absolute direction does not vary significantly, then the direction $\phi(Z)$ of the relative wind may vary considerably over the height of the sail (figure 3).

2.2. *Induced velocities due to the trailing vortex sheet*

The presence of a trailing vortex sheet gives rise to induced velocities in the surrounding flow. In general, these velocities have vertical components as well as horizontal components. However, at the horizontal water surface, which for the purpose of the present analysis is assumed to be flat, the vertical component must obviously be zero. This is achieved by means of an image sail to give symmetry about the water surface plane.

It can be shown that the integrated effect of the semi-infinite sheet of trailing vortex elements of strength $\dot{\Gamma}(Z')$ [see (1)] and inclined at an angle $\phi(Z)$ to the yacht centreline gives rise to a horizontal induced velocity at any height Z on the vertical sail axis (see figure 2). This velocity has components $U_i(Z)$ in the X (forward) direction and $V_i(Z)$ in the Y direction given by

$$U_i(Z) = \frac{1}{4\pi}\int_0^H \dot{\Gamma}(Z')\sin\phi(Z')\left\{\frac{1}{Z'-Z}+\frac{1}{Z'+Z}\right\}dZ', \tag{2}$$

$$V_i(Z) = \frac{1}{4\pi}\int_0^H \dot{\Gamma}(Z')\cos\phi(Z')\left\{\frac{1}{Z'-Z}+\frac{1}{Z'+Z}\right\}dZ'. \tag{3}$$

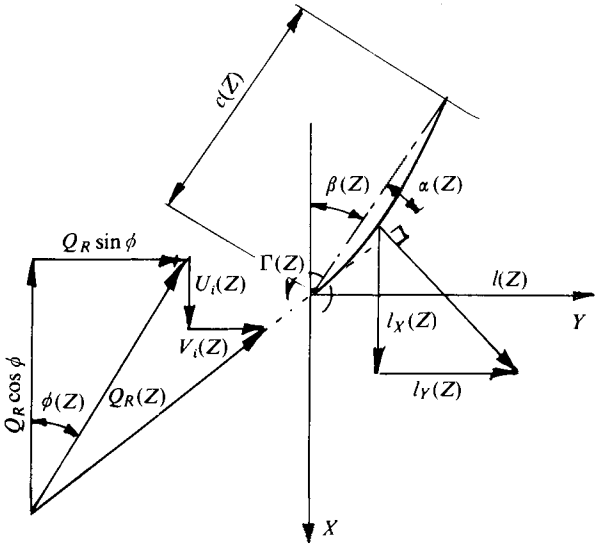

FIGURE 4. Velocity and force vectors.

2.3. *Aerodynamic forces and moments*

To calculate the aerodynamic force, normally known as lift, normal to a stream of velocity Q when it flows over an aerofoil having circulation Γ, use is made of the Blasius theorem, which leads to the result

$$L = \rho Q \Gamma.$$

This two-dimensional result has been extended for use on finite wings where Γ is a variable, and also propeller blades where neither Q nor Γ remains constant, by applying the equation locally at every section. To do this it is simply necessary to recognize that the direction of the local force per unit span is at right angles not just to the undisturbed free stream, but to the locally deflected stream including the induced effects of the trailing vortex system. In the case of a sail in a non-uniform wind the same approach is equally valid. Thus in the present case we refer to figures 3 and 4 and write the local force components $l_X(Z)$, $l_Y(Z)$ per unit height of the sail as

$$l_X(Z) = \rho\{Q_R(Z)\sin\phi(Z) + V_i(Z)\}\,\Gamma(Z), \tag{4}$$

$$l_Y(Z) = \rho\{Q_R(Z)\cos\phi(Z) - U_i(Z)\}\,\Gamma(Z). \tag{5}$$

These local force components may then be integrated over the whole height of the sail in order to determine the overall wind force components:

$$F_X = \int_0^H l_X(Z)\,dZ = \rho\int_0^H \{Q_R(Z)\sin\phi(Z) + V_i(Z)\}\,\Gamma(Z)\,dZ, \tag{6}$$

$$F_Y = \int_0^H l_Y(Z)\,dZ = \rho\int_0^H \{Q_R(Z)\cos\phi(Z) - U_i(Z)\}\,\Gamma(Z)\,dZ. \tag{7}$$

With the sign convention shown in figure 4 the forward thrust on the yacht is F_X while F_Y is the lateral force which must be resisted by the 'lift' on the keel and underwater surfaces of the hull as it moves through the water. See also figure 5.

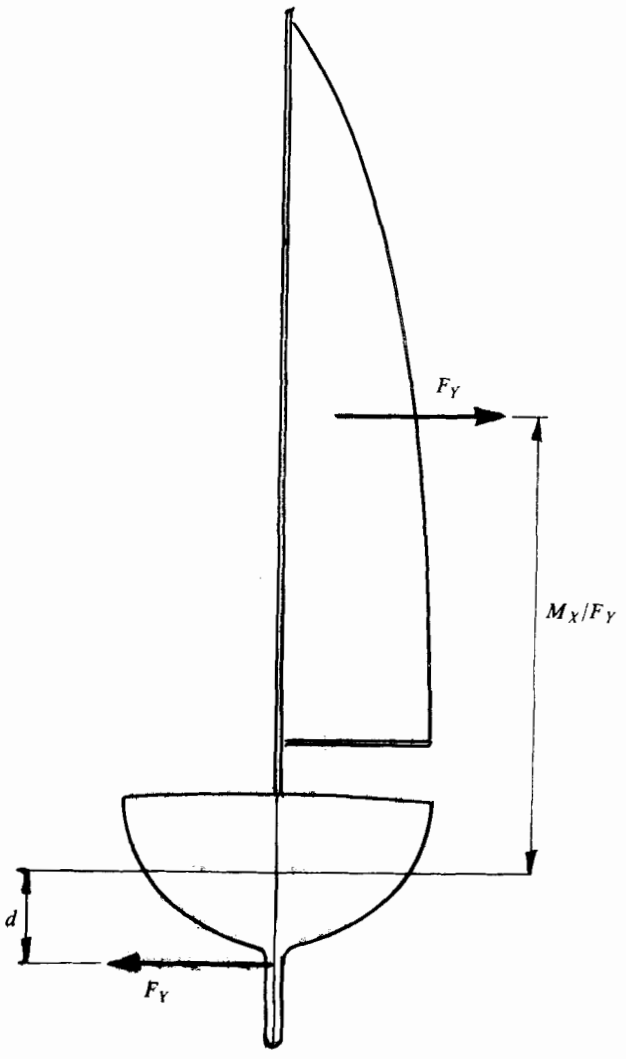

FIGURE 5. Definition of rolling moment M_X.

Of equal importance of course is the capacity of the hull to resist a rolling moment without heeling excessively or capsizing. If the side force F_Y is resisted by the hull at an effective depth d below the surface (figure 5) then the total rolling moment M_R may be described by

$$M_R = -M_X + F_Y d,$$

where M_X is the moment of the lateral wind force about $Z = 0$,

$$M_X = -\int_0^H Z l_Y(Z)\, dZ = -\rho \int_0^H \{Q_R(Z)\cos\phi(Z) - U_i(Z)\}\,\Gamma(Z)\, Z\, dZ.$$

Since it is the purpose of the present analysis to consider sail design only and to avoid any involvement with hull interactions, it will be assumed that $F_Y d \ll M_X$. This statement is probably quite accurate in the case of catamarans, but the relatively deep keel on most monohull craft probably increases significantly the effective

moment arm associated with a given side force. For this reason, despite some loss in performance, dinghy sailors sometimes find an improvement in comfort if the centre-board is not extended to its full depth when sailing to windward in strong winds. Neglecting this unspecified keel moment for the present, we may write

$$M_R \doteq \rho \int_0^H \{Q_R(Z)\cos\phi(Z) - U_i(Z)\}\,\Gamma(Z)\,Z\,dZ. \tag{8}$$

Pitching moments (especially important in catamaran design) and the effects of roll angle including yawing moments are not a necessary topic for inclusion in the present argument. A more general and comprehensive analysis of yacht sails including the effects of roll has been published by Milgram (1968).

3. Real effects and limitations of the analysis

3.1. *Description of sail geometry*

The present description of the aerodynamic effect of a yacht sail in terms of a mere circulation distribution $\Gamma(Z)$ is all that is necessary for the proposed optimization calculation. However it may assist the physical interpretation, and of course the ultimate application of the results, if the sail can also be considered as a physical shape with chord $c(Z)$ and a curvature which produces a lift coefficient $C_L(Z)$ at an angular setting $\beta(Z)$ relative to the yacht centre-line.† This is accomplished by noting that

$$C_L(Z) = l(Z)/\{\tfrac{1}{2}\rho Q_R^2(Z)\,c(Z)\}$$

while

$$l(Z) = \{l_X^2(Z) - l_Y^2(Z)\}^{\frac{1}{2}} = \rho Q_R(Z)\,\Gamma(Z).$$

Thus

$$C_L(Z) = 2\Gamma(Z)/Q_R(Z)\,c(Z).$$

The curved shape and angular position of the sail may be included in the description by applying locally the standard result of two-dimensional thin-aerofoil theory that any curved camber line has a design lift coefficient $C_{L0}(Z)$ at a particular design incidence $\alpha_0(Z)$ relative to the oncoming free stream.

At any other incidence $\alpha(Z)$ this shape has a modified lift coefficient given by

$$C_L(Z) = C_{L0}(Z) + 2\pi\{\alpha(Z) - \alpha_0(Z)\}.$$

As a result of induced velocity components, the relative air stream is inclined to the yacht centre-plane not at $\phi(Z)$ but at a modified angle $\phi(Z) + \epsilon(Z)$ given by

$$\tan\{\phi(Z) + \epsilon(Z)\} = \{Q_R(Z)\sin\phi(Z) + V_i(Z)\}/\{Q_R(Z)\cos\phi(Z) - U_i(Z)\},$$

so that the inclination of the sail to the yacht axis is given by

$$\beta(Z) = \phi(Z) + \epsilon(Z) - \alpha(Z).$$

3.2. *Defects of lifting-line theory*

Strictly, of course, these statements about sail shape are quite inconsistent with the use of lifting-line theory, which, by definition, is incapable of describing the near flow field correctly. The description is not used in the present analysis. Its value is simply

† This is of course a very elementary description. Analyses which take account of sail flexibility have been performed, notably by Thwaites (1961) and Duggan (1966).

that it emphasizes the practical fact that a circulation distribution $\Gamma(Z)$ cannot be generated without a lifting surface of finite size $c(Z)$ shaped and inclined to produce a finite and limited local lift coefficient $C_L(Z)$. Both these features are reminders of the profile drag, which varies both with the surface area and with the lift coefficient.

By neglecting this variable drag contribution, the present analysis not only overestimates the thrust, but also produces an artificially simple statement of its variation. This must be recognized when assessing the results.

Errors which are of second order and therefore of much less significance include the fact that the trailing vortex sheet does not extend to infinity in practice but rolls up to form discrete tip vortices. Also, the real trailing vortex pattern, having a self-induced transverse velocity, does not lie quite parallel to the undisturbed approaching flow. The use of $\sin\phi(Z')$ and $\cos\phi(Z')$ in (2) and (3) is therefore slightly in error.

3.3. *Hull disturbance and gap effects*

Following Tanner (1965) and Milgram (1968), an attempt is made in the present analysis to include an elementary description of the gap below the foot of the sails. However, the gap thus represented contains no simulation of the hull of the boat, which partially obstructs that gap.

It is of course as inconsistent in the context of lifting-line theory to consider the detailed shape of the hull as it is to consider the detailed shape of the sails. An appropriate modification to the theory might be to locate the gap some way above the water surface and to apply a loading distribution to represent the hull. Failing this it must be recognized that a cross-flow over the hull probably has the beneficial effect of increasing the effective incidence of the sail at low levels.

The disadvantage of the gap remains severe however as the present results show and it is perhaps not inappropriate to refer to the popularity of the low-cut Genoa jib among racing yachtsmen and to suggest that practical efforts can and should be made to reduce the size of the gap.

It is debatable whether the present argument is helped by including the effect of a gap when so many other real effects are ignored. Indeed, since the primary objective of the analysis is to compare a new optimization criterion with the conventionally accepted maximization of the lift–drag ratio, it is most important to apply the same restrictions to the former as to the latter.

The earlier analysis, applied of course to aeroplanes, has no gap, neither is it influenced in any way by fuselage cross-flow effects. Consequently the only valid comparison is with an analysis which makes the same assumptions however unrealistic these may be. To achieve this direct comparison the present analysis is repeated in §7 with the gap removed.

4. Optimization criterion and dimensionless equations

As previously stated, the aim of the present paper is to consider whether there exists a theoretical optimum sail. In order to pursue this objective it is necessary to define what is meant by an optimum sail and to consider what constraints, if any, are to be applied as the optimum is determined. For example, a restricted mast height might lead to a very different optimum from that which would be discovered if the total sail area were limited instead.

For the purpose of the present argument, all limitations based upon conventional yacht racing class rules, and even upon safety or engineering practicability, are removed in order to ask in a totally uninhibited way the question: 'what sort of sail will provide the greatest possible forward thrust for a given hull when sailing to windward?'

The question has been posed deliberately in terms of forward thrust rather than forward speed in order to avoid, for the present, any consideration of hull-dynamic effects. This is unrealistic in that the induced drag of the underwater parts of the hull will certainly increase with increasing side force. However, provided that this is remembered when assessing the results, it is sufficient for the present purpose to think of the hull simply in terms of its capacity to resist the rolling moment generated by the sail.

When considered in this way the optimum sail is clearly one which generates the largest possible thrust F_X without exceeding some fixed limiting value of the rolling moment M_R.

To simplify the present results still further, the number of variables affecting the forward thrust is reduced by assuming that the incident relative wind vector $(Q_R(Z), \phi(Z))$ is uniform. This assumption also removes the only obstacle to a truly dimensionless and therefore general formulation of the problem (Wood & Tan 1976). A further benefit is that the direct comparison with other results, discussed in the previous section, remains possible inasmuch as these also assume uniform flow.

It is essential, in any dimensionless formulation of the present problem, to retain the dimensionless mast height h as an independent variable. The rolling moment M_R, on the other hand, is specified as being a constant and equal to the limiting rolling moment M_0 which the hull can withstand. Under these conditions, dimensional analysis reveals an alternative constant reference length l_0 defined by

$$l_0 = (M_0/\rho Q_R^2)^{\frac{1}{3}}.$$

The remaining dimensionless parameters are then given as follows:

$$f_X = F_X/(\rho Q_R^2 l_0^2), \quad f_Y = F_Y/(\rho Q_R^2 l_0^2),$$

$$M_r = M_R/(\rho Q_R^2 l_0^3) = M_R/M_0,$$

$$h = H/l_0, \quad g(z) = \Gamma(Z)/(Q_R l_0).$$

For convenience in the subsequent Fourier analysis the dimensionless position variable z is still defined with reference to the mast height H rather than l_0, i.e.

$$z = Z/H, \quad b = B/H.$$

Using these variables, (6) and (7) may be rewritten as

$$f_x = h\int_0^1 \{\sin\phi + q_i(z)\cos\phi\}\, g(z)\, dz, \tag{9}$$

$$f_Y = h\int_0^1 \{\cos\phi - q_i(z)\sin\phi\}\, g(z)\, dz, \tag{10}$$

where the induced velocity components are defined by (2) and (3) such that

$$q_i(z) = \frac{U_i^2(Z) + V_i^2(Z)}{Q_R^2} = \frac{1}{4\pi h}\int_0^1 \dot{g}(z')\left\{\frac{1}{z'-z} + \frac{1}{z'+z}\right\} dz'. \tag{11}$$

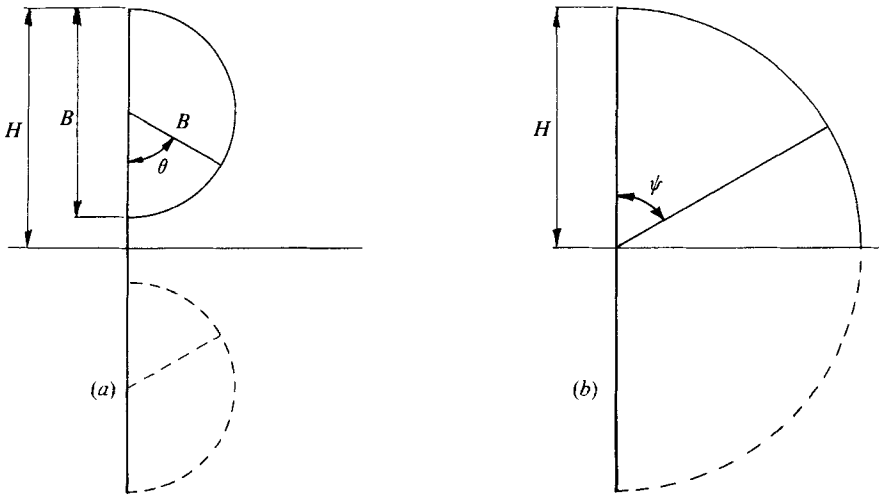

FIGURE 6. Co-ordinate transformations for Fourier series.
(*a*) Sail with gap. (*b*) Sail with no gap.

Because the reference length l_0 is related to the limiting hull rolling moment M_0 the requirement that the rolling moment M_R of the sail shall not exceed this limiting value corresponds to the statement $m_r \leqslant 1$. Thus (8) leads to a dimensionless relationship which sets a limit upon the circulation strength in terms of the mast height:

$$1 \geqslant h^2 \int_0^1 \{\cos\phi - q_i(z)\sin\phi\} z g(z)\, dz. \tag{12}$$

5. Fourier series for circulation

In (9)–(12) the circulation distribution $g(z')$ is not yet determined. The aim of the present analysis is in fact to specify a circulation distribution which will maximize the value of f_x in (9) whilst satisfying the rolling-moment limitation described in (12).

It is obvious physically that $g(z')$ must be zero both at the head and at the foot of the sail. Thus a convenient Fourier representation for $g(z)$ is an odd (sine terms only) series based upon an angle parameter which is zero at the foot of the sail and which reaches a value π at the head. A suitable co-ordinate transformation is shown in figure 6(*a*), where the luff of the sail has length B. This, and the subsequent analysis leading to (15)–(17), is essentially similar to that used by Tanner (1965):

$$Z = H - \tfrac{1}{2}B - \tfrac{1}{2}B\cos\theta.$$

Using this transformation in dimensionless form we have

$$z = 1 - \tfrac{1}{2}b - b\cos\theta$$

with a corresponding equation for the dummy variable z' in terms of θ', so that

$$z' - z = -\tfrac{1}{2}b(\cos\theta' - \cos\theta)$$

and

$$z' + z = \tfrac{1}{2}b(a - \cos\theta'),$$

where

$$a = 4/b - 2 - \cos\theta.$$

If the Fourier series for $g(z')$ is then written as

$$g(z') = \sum_{n=1}^{\infty} A_n \sin n\theta'$$

we may substitute in (11) to obtain the induced velocity

$$q_i(z) = \frac{1}{2\pi hb} \sum_{n=1}^{\infty} nA_n \left\{ -\int_0^{\pi} \frac{\cos n\theta' d\theta'}{\cos\theta' - \cos\theta} + \int_0^{\pi} \frac{\cos n\theta'\, d\theta'}{a - \cos\theta'} \right\}.$$

Evaluating the integrals, we have finally

$$q_i(z) = \frac{1}{2hb} \sum_{n=1}^{\infty} nA_n \left\{ -\frac{\sin n\theta}{\sin\theta} + \frac{[a - (a^2-1)^{\frac{1}{2}}]^n}{(a^2-1)^{\frac{1}{2}}} \right\}. \tag{13}$$

With the same substitution in (9) we have

$$\begin{aligned} f_x = {} & \frac{hb\sin\phi}{2} \int_0^{\pi} \sum_{n=1}^{\infty} A_n \sin n\theta \sin\theta\, d\theta \\ & - \frac{\cos\phi}{4} \int_0^{\pi} \sum_{m=1}^{\infty} mA_m \sin m\theta \sum_{n=1}^{\infty} A_n \sin n\theta\, d\theta \\ & + \frac{\cos\phi}{4} \int_0^{\pi} \sum_{m=1}^{\infty} mA_m \frac{[a - (a^2-1)^{\frac{1}{2}}]^m}{(a^2-1)^{\frac{1}{2}}} \sum_{n=1}^{\infty} A_n \sin n\theta \sin\theta\, d\theta. \end{aligned}$$

After evaluating the integrals, this reduces to

$$f_x = \frac{\pi hb\sin\phi}{4} A_1 - \frac{\pi\cos\phi}{8} \sum_{n=1}^{\infty} n A_n^2 + \frac{\cos\phi}{4} \sum_{m,n=1}^{\infty} mA_m A_n E_1(m,n),$$

where

$$E_1(m,n) = \int_0^{\pi} \frac{[a - (a^2-1)^{\frac{1}{2}}]^m}{(a^2-1)^{\frac{1}{2}}} \sin n\theta \sin\theta\, d\theta. \tag{15}$$

Similarly (10) becomes

$$f_y = \frac{\pi hb\cos\phi}{4} A_1 + \frac{\pi\sin\phi}{8} \sum_{n=1}^{\infty} nA_n^2 - \frac{\sin\phi}{4} \sum_{m,n=1}^{\infty} mA_m A_n E_1(m,n) \tag{16}$$

while (12) reduces to†

$$\begin{aligned} 1 = {} & \frac{\pi h^2 b(2-b)\cos\phi}{8} A_1 - \frac{\pi h^2 b^2 \cos\phi}{16} A_2 \\ & + \frac{\pi h(2-b)\sin\phi}{16} \sum_{n=1}^{\infty} nA_n^2 - \frac{\pi hb\sin\phi}{32} \sum_{n=1}^{\infty} nA_n (A_{(n-1)} + A_{(n+1)}) \\ & - \frac{h(2-b)\sin\phi}{8} \sum_{m,n=1}^{\infty} mA_m A_n E_1(m,n) + \frac{hb\sin\phi}{16} \sum_{m,n=1}^{\infty} mA_m A_n E_2(m,n), \end{aligned} \tag{17}$$

† The fourth term in (17) may be written in this form provided that A_{n-1} is taken to be zero when $n = 1$.

where $E_1(m, n)$ is as previously defined and

$$E_2(m, n) = \int_0^{\pi} \frac{[a - (a^2 - 1)^{\frac{1}{2}}]^m}{(a^2 - 1)^{\frac{1}{2}}} \sin n\theta \sin 2\theta \, d\theta. \tag{18}$$

6. Numerical evaluation

The task of choosing a set of Fourier coefficients A_n which maximizes the value of f_x [equation (14)] whilst satisfying the rolling-moment limitation [equation (17)] was carried out numerically from this point, using the I.C.L. 1906 computer of the Oxford University Computing Service.

It was planned initially to use up to fifteen terms in a truncated Fourier series, but after some trials it was found that this number could be reduced to ten without significant loss of accuracy.

Before computing each case, values of the dimensionless mast height h, the luff length fraction b and the relative wind angle ϕ were chosen as constants. Using these values, the twelve constant coefficients in (14), (16) and (17) were then calculated. Also, arrays of values for the integrals $E_1(m, n)$ and $E_2(m, n)$ were prepared according to (15) and (18) using Simpson's rule.

As an arbitrary starting point for the optimization procedure, all the Fourier coefficients except the first were assigned zero values. This reduced (17) to a quadratic expression yielding a starting value for A_1, which could be substituted in (14) to determine a base value for f_x.

A trial value of the next Fourier coefficient A_2 was then introduced. When combined with the starting value of A_1 in (17) this yielded a value of the rolling moment which was no longer unity. The next operation was therefore to determine a scaling factor which, when applied to every coefficient, would produce a new set of coefficients giving unit rolling moment and thus satisfying (17). By using these new values of A_1 and A_2 in (14) a revised value of f_x was produced. A comparison between this and the previous value showed whether or not the latest change in A_2 constituted an improvement. In the light of this information the next and subsequent changes in A_2 were modified until a maximum in f_x was detected.

This cycle was repeated in order to introduce and optimize each successive Fourier coefficient in turn until all ten coefficients had been determined. These were then used finally to describe the loading distribution and to evaluate the associated side thrust f_y from (16).

An obvious fault in this procedure is that it does not necessarily satisfy the requirement for simultaneous optimization of all the coefficients. To investigate this difficulty, a convergence check was run in a number of cases. This was done by repeating the term-by-term optimization but starting with initial values taken fron the previous solution. In the cases tested, the variation in f_x as a result of this second approximation was of order 0·1 only and it was judged that a second approximation was not necessary.

7. A reference case: zero gap and elliptic loading

A simple presentation of the results of (14) and (17) makes no impact because it contains no demonstration that the present optimum loading distribution gives

improved performance. A reference condition is required for the purpose of comparison.

The obvious reference case is the minimum-drag, elliptic-loading condition, which has often been regarded as the best for windward performance. This is defined as a continuous distribution with no gap and with symmetry about the plane of the water surface. Because the zero-gap condition is a failing case in the equations used above, a modified analysis is required in order to achieve an adequate description.

In this modified analysis we replace (2) and (3) by a form which does not involve the simultaneous consideration of a trailing vortex element and its image but which integrates instead over a double-sided distribution which includes both the real sail and its image so that

$$U_i(Z) = \frac{1}{4\pi}\int_{-H}^{H} \frac{\dot{\Gamma}(Z')\sin\phi(Z')\,dZ'}{Z'-Z}, \tag{2a}$$

$$V_i(Z) = \frac{1}{4\pi}\int_{-H}^{H} \frac{\dot{\Gamma}(Z')\cos\phi(Z')\,dZ'}{Z'-Z}. \tag{3a}$$

When written in terms of the dimensionless variables previously defined, (2*a*) and (3*a*) lead to a modified version of (11), namely

$$q_i(z) = \frac{1}{4\pi h}\int_{-1}^{1} \frac{g(z')\,dz'}{z'-z}. \tag{11a}$$

The force and moment equations (9), (10) and (12) are unchanged.

To represent a loading distribution which is continuous through the water surface and which is symmetrical about $z = 0$, it is convenient to use a Fourier series based upon the modified co-ordinate transformation

$$z = \cos\psi.$$

The loading distribution must then be made up of the symmetrical or odd terms in the Fourier sine series

$$g(z') = \sum_{m=1}^{\infty} A_j \sin j\psi',$$

where $j = 2m-1$. With this substitution, (11*a*) becomes

$$q_i(z) = -\frac{1}{4\pi h}\int_0^{\pi} \frac{\sum_{m=1}^{\infty} jA_j \cos j\psi\, d\psi}{\cos\psi' - \cos\psi}.$$

After integration we have an equation for the induced velocity to replace (13):

$$q_i(z) = -\frac{1}{4h}\sum_{m=1}^{\infty} jA_j \sin j\psi/\sin\psi. \tag{13a}$$

Substituting the appropriate components of this induced velocity in (9), (10) and (12) and noting that an integral over the height of the real sail now corresponds to an integral from $\psi = \frac{1}{2}\pi$ to $\psi = 0$ in the modified co-ordinates, the following relationships are obtained:

$$f_x = h\sin\phi\int_0^{\frac{1}{2}\pi}\sum_{m=1}^{\infty} A_j \sin j\psi\sin\psi\,d\psi$$

$$-\frac{\cos\phi}{4}\int_0^{\frac{1}{2}\pi}\sum_{m=1}^{\infty} jA_j \sin j\psi \sum_{n=1}^{\infty} A_k \sin k\psi\,d\psi,$$

$$f_y = h\cos\phi \int_0^{\frac{1}{2}\pi} \sum_{m=1}^{\infty} A_j \sin j\psi \sin\psi \, d\psi + \frac{\sin\phi}{4} \int_0^{\frac{1}{2}\pi} \sum_{m=1}^{\infty} jA_j \sin j\psi \sum_{n=1}^{\infty} A_k \sin k\psi \, d\psi,$$

$$1 = h^2\cos\phi \int_0^{\frac{1}{2}\pi} \sum_{m=1}^{\infty} A_j \sin j\psi \sin\psi \cos\psi \, d\psi + \frac{h\sin\phi}{4} \int_0^{\frac{1}{2}\pi} \sum_{m=1}^{\infty} jA_j \sin j\psi \sum_{n=1}^{\infty} A_k \sin k\psi \cos\psi \, d\psi,$$

where $$j = 2m-1 \quad \text{and} \quad k = 2n-1.$$

Because j and k are both odd numbers, all the terms in these integrals are symmetrical about $\psi = \frac{1}{2}\pi$ ($z = 0$). In every case, therefore, we may replace the half-span (0 to $\frac{1}{2}\pi$) integral by one half of the full-span (0 to $\frac{1}{2}\pi$) integral. The use of full-span integrals makes it possible to invoke a standard integral result and obtain the final expressions for the forward thrust f_x and the side thrust f_y which replace (14) and (16):

$$f_x = \frac{\pi h \sin\phi}{4} A_1 - \frac{\pi\cos\phi}{16} \sum_{m=1}^{\infty} jA_j^2, \tag{14a}$$

$$f_y = \frac{\pi h\cos\phi}{4} A_1 + \frac{\pi\sin\phi}{16} \sum_{m=1}^{\infty} jA_j^2. \tag{16a}$$

The rolling-moment equation is treated slightly differently to give

$$1 = h^2\cos\phi \sum_{m=1}^{\infty} A_j E(j,1) + \frac{h\sin\phi}{4} \sum_{m,n=1}^{\infty} jA_j A_k E(j,k), \tag{17a}$$

where

$$\begin{aligned} E(j,k) &= \int_0^{\frac{1}{2}\pi} \sin j\psi \sin k\psi \cos\psi \, d\psi \\ &= \frac{1}{4}\left\{\frac{\sin\frac{1}{2}(j-k-1)\pi}{j-k-1} + \frac{\sin\frac{1}{2}(j-k+1)\pi}{j-k+1} - \frac{\sin\frac{1}{2}(j+k-1)\pi}{j+k-1} - \frac{\sin\frac{1}{2}(j+k+1)\pi}{j+k+1}\right\} \\ &= (-1)^{\frac{1}{2}(j+k)}(j^2+k^2-1)/\{[(j-k)^2-1][(j+k)^2-1]\}. \end{aligned} \tag{18a}$$

The reference case of elliptic loading is of course obtained by setting all the Fourier coefficients to zero except the fundamental coefficient A_1 and determining the value of A_1 which satisfies (17a).

If further coefficients are included, these may be optimized by precisely the same numerical procedure as that described in §6 in order to show, for the zero-gap case, the extent of the improvement which can be obtained in forward thrust compared with that given by elliptic loading.

8. Results and discussion

8.1. *Motivation*

When considering the results of the present calculations it must be remembered that, in using lifting-line theory, an artificially simple and unrealistic model has been chosen to represent the flow of wind over yacht sails. This, together with the omission of several important effects discussed in §§2.3, 3 and 4, is done deliberately in order to

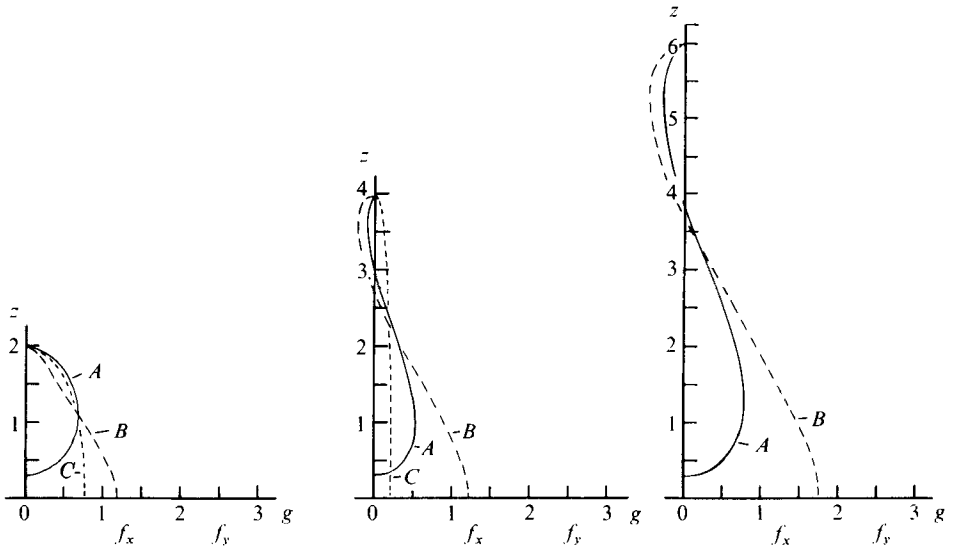

	f_x	f_y
A	0·233	0·887
B	0·438	1·395
C	0·414	1·179

	f_x	f_y
A	0·281	0·810
B	0·487	1·610
C	0·266	0·589

	f_x	f_y
A	0·366	1·320
B	0·710	2·841
C	0·181	0·393

FIGURE 7. Circulation distributions for $\phi = 25°$. *A*, optimum loading with boom height 0·3; *B*, optimum loading with zero gap; *C*, elliptic loading.

achieve the degree of generality afforded by a simple dimensionless presentation and also to allow a direct comparison with elliptic loading. This is the well-known result of lifting-line theory which corresponds to maximum lift–drag ratio. In their continuing attempts to improve the lift–drag ratio, modern sail designers have sought to realize the theoretically predicted benefits of sail plans of high aspect ratio. They have also succeeded to a remarkable degree in controlling the curvature and twist of flexible sails to produce loading distributions which approximate as closely as possible to the elliptical form.

These practical advances were achieved when designers, having become aware of a theoretical target (albeit an unrealistic one), sought realistic ways of approaching that target. In the confidence that this remains a valid method for attempting design improvements, the present paper sets out to demonstrate, by means of a direct comparison using the same theory, that a rather different optimum sail loading may yield advantages over the elliptic form in circumstances where there exists only a rolling-moment constraint.

8.2. *Description of results*

Calculated results are presented in figures 7 and 8 for relative wind angles of 25°, which is rather extreme for close-hauled sailing, and 45°, which represents a comfortable close reach. The luff length ratio b is chosen in each case to give the same dimensionless boom height of 0·3 on the mast-height scale. To appreciate the physical significance of the variation in h from 2 to 6, a comparison may be made with a typical racing dinghy having a rolling-moment limitation of 1500 N m, obtained mainly by disposition of the crew weight, and a mast height of 7 m. In a wind of speed 10 m/s this situation corresponds to a value of 3·05 for the dimensionless mast height h.

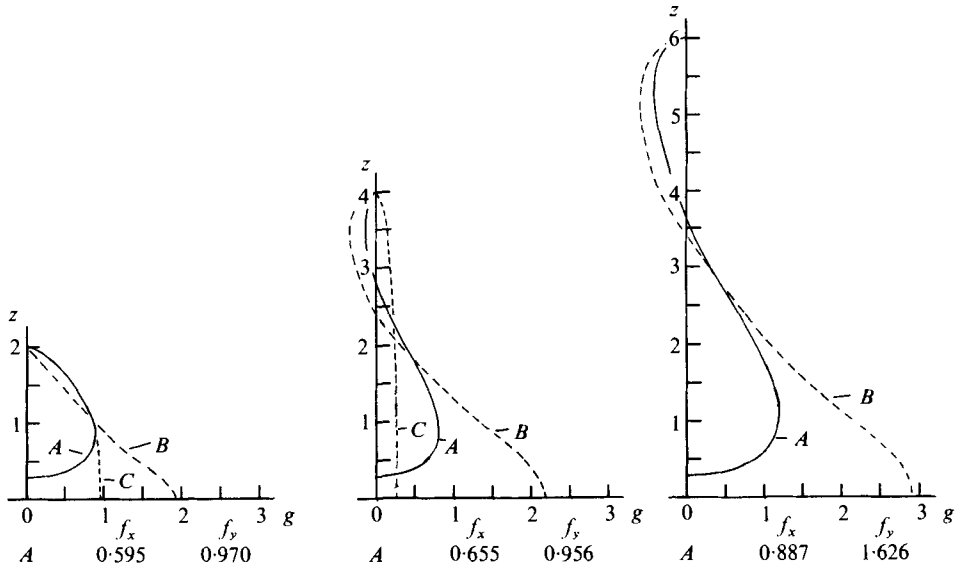

	f_x	f_y
A	0·595	0·970
B	1·078	1·693
C	0·929	1·179

	f_x	f_y
A	0·655	0·956
B	1·210	2·193
C	0·571	0·589

	f_x	f_y
A	0·887	1·626
B	1·805	3·737
C	0·389	0·411

FIGURE 8. Circulation distributions for $\phi = 45°$. *A*, optimum loading with boom height 0·3; *B*, optimum loading with zero gap; *C*, elliptic loading.

Clearly, therefore, to extend the present calculations to $h = 6$ is to adventure wildly beyond the limits of present-day design. However, the value of such extravagance will be more than proved if the novel thoughts provoked by these results lead, even occasionally, to imaginative experiments.

On each graph, case *A* represents the optimum loading distribution with an under-boom gap. In case *B* that gap is removed in order to compare more directly with case *C*, where the inclusion of the first Fourier coefficient alone leads to the classical case of elliptic loading. In the tallest case, the elliptic distribution is not plotted; the ordinates are too small.

Beneath each loading diagram are tabulated the associated values of the forward thrust f_x and the side thrust f_y.

8.3. *Interpretation*

Examining first the very conservative case $h = 2$, it is clear that, for low sail plans or light winds elliptic loading yields comparable performance with the optimum form. Thus the present analysis has little to offer. However as h increases to 4 it is clear that the optimum loading yields a thrust improvement associated with a very much reduced lift derived from the upper part of the sail. Conventional reefing of course achieves this crudely. A better example, however, is found in the practice of those dinghy helmsmen who so arrange their sheets and boom downhaul devices that the top of the sail is allowed to twist to leeward when beating in uncomfortably strong winds.

It is when the extreme cases ($h = 6$) are examined that the physical significance of these results really becomes outstandingly clear. Here, because of the disproportionate overturning effect of a conventionally loaded sail, the magnitude of the elliptic

loading distribution becomes very small and the corresponding forward thrust is severely reduced (not to mention the windage effect of a tall mast relative to a very slender sail). By contrast, the optimum loading is able to carry an increased lift, either by increased incidence or extended sail area, over a large proportion of the sail and thus produces a considerably increased thrust. The striking observation is that this is achieved in association with an actual *reversal* of lift at the top of the sail. Thus the top of the sail is not used to produce thrust. A1 negative incidence the local force vector will be inclined decidedly backwards. Instead, the negative-lift portion has the effect, by virtue of the associated long moment arm, of holding the craft upright, at the expense of some drag, in order to support a very much increased sail loading lower down.

8.4. *Applications*

If an attempt is made to translate this observation into practical terms, then the implication is that it may be advantageous to design very tall masts, or very light and tender hulls, and to incorporate a means of actually forcing the upper portion of the sail to leeward. Negative lift could then be produced when necessary in order to balance the vessel in very strong winds.

Should it ever become possible to overcome the severe structural and control problems associated with this proposal, then it would appear that significant increases in performance might be gained. The numbers produced by the present over-simplified calculations should of course be regarded as optimistic. The inclusion of the gap case illustrates this by showing how one particular improvement in realism reduces the calculated advantage of optimization. Nevertheless, some real effects such as the gap, hull cross-flow roll angle or wind sheer are ignored equally in both the elliptic and the optimum case. These therefore are unlikely to alter the present conclusion.

The effects which will reduce the benefits of optimization are those where optimization itself creates, but does not take into account, greater losses than those associated with the elliptic case. The greatly increased side thrust is a serious example. This must be supported by the lift of the underwater parts of the hull. Consequently these must be either increased in size, yielding greater skin-friction drag, or operate in a more highly loaded condition with a consequent penalty in underwater induced drag.

In the same way the required increase in sail lift may be achieved by increasing either the area or the local lift coefficient. Both effects carry a drag penalty which will reduce the benefits of the optimization.

8.5. *Other work*

Once the present analysis is applied in the context of a particular design, then it becomes possible of course to include many of these effects and thus improve the realism of the calculation. This has been attempted by Wood (1971, unpublished calculation) and also by Perkins (1977) with results which remain encouraging.

Of similar interest is a somewhat incomplete experiment described by Gopal (1977). The project, undertaken at model scale in a wind tunnel, was to measure the forward thrust on a rigid sail of symmetrical 21 % thick section when the tip was controlled to rotate as necessary to maintain a fixed root bending moment about the roll axis of the simulated hull. The fact that an electronic control system was required to adjust the tip incidence stands as an example of the practical engineering problems associated with the present suggestions.

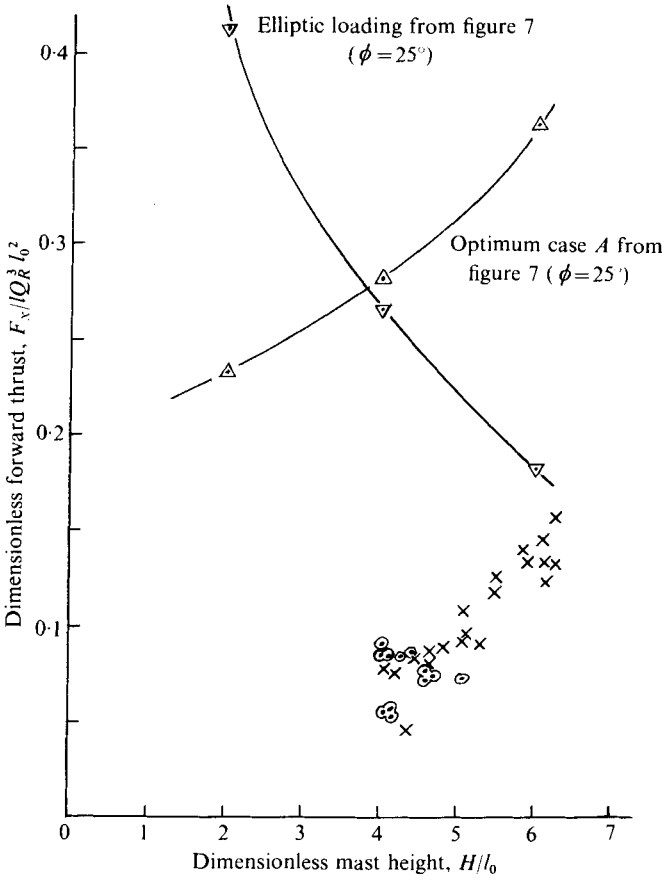

FIGURE 9. Comparison with experimental result by Gopal (1977). ○, Gopal, untwisted (ϕ = 30°); ×, Gopal, active tip (ϕ = 30°).

After setting the 'yacht axis' at a suitable 'course angle' and the main part of the sail at a fixed incidence, the wind speed was slowly increased while the forward thrust was measured by a strain-gauge balance in the sail root. With the control system inoperative, the limiting wind speed and hence the limiting forward thrust value was achieved when the capsize condition was observed at a pre-set rolling moment. The experiment was then repeated with the control system active. After the limiting wind speed was exceeded, Gopal reports a visible variation in the angle of the movable sail tip, a constant value of the rolling moment and a thrust value in excess of the previous maximum and increasing with speed.

Figure 9 shows Gopal's forward-thrust measurements, recalculated in the present dimensionless form. Unfortunately Gopal selected a course angle of 30°. Nevertheless a comparision is made with the present 25° thrust values from figure 7.

The comparison illustrates of course the extent to which practical results are lower than the predictions of the lifting-line model. Nevertheless it also shows quite clearly, despite the large experimental scatter, that a simple rotation of the top of the experimental sail has produced an increase in thrust with an increase in h, which is similar to the trend predicted for the optimum-loading case. The maximum experimental

thrust achieved was approximately double the value available from the untwisted sail subject to the same rolling-moment limitation.

The comparison between this simple experiment and the present dimensionless statements is not a direct one. The wing planform was rectangular and the twist was a step function, so neither elliptic loading nor the present optimum are relevant descriptions of the flow. Nevertheless, as the only experimental evidence relating to the present problem, the qualitative support it provides is encouraging. It is hoped that further experimental results will be forthcoming.

REFERENCES

DUGGAN, J. P. 1966 *J. Fluid Mech.* **42**, 433–446.
GOPAL, I. S. 1977 *Oxford Univ. Undergrad. Proj. Rep.*
MILGRAM, J. H. 1968 *7th Symp. Naval Hydrodyn. Rome.*
PERKINS, P. H. 1977 *Oxford Univ. Undergrad. Proj. Rep.*
TAN, S. H. 1976 *Oxford Univ. Undergrad. Proj. Rep.*
TANNER, T. 1965 *Southampton Univ. Yacht Res. Rep.* no. 16.
THWAITES, B. 1961 *Proc. Roy. Soc.* A **261**, 402–422.
WOOD, C. J. & TAN, S. H. 1976 *Oxford Univ. Engng Lab. Rep.* no. 1164/76.